Lattice Dynamics of Copper at 80 K

G. Nilsson and S. Rolandson

AB Atomenergi, Studsvik, Sweden

(Received 15 November 1971)

Phonon frequencies of copper have been measured at 80 K with a neutron crystal spectrometer at a large number of points—mainly in off-symmetry directions. The frequency distribution is calculated, and also the Debye temperature in the interval 0-300 K. The agreement with calorimetric measurements is very satisfactory. Several Born–von Kármán models were fitted to the experimental frequencies. The best fit was obtained using a model with general forces extending to eighth nearest neighbors. The conditions for axial symmetry of the interatomic forces are much better fulfilled in copper than, for instance, in aluminum. However, a general force model is preferable also for copper when a good fit in the whole zone is wanted.

I. INTRODUCTION

It is a common routine in studies of lattice dynamics of metals to measure the phonon-dispersion curves in the symmetry directions, and then fit force-constant models to the measured frequencies. The force constants are sometimes assumed to have a real physical meaning; sometimes they are used only as a means of obtaining interpolation formulas for the calculation of phonon frequencies, frequency distribution, and polarization vectors. By assuming certain conditions for the relations between some of the constants, one may include forces from remote neighbors and derive curves which give a very good fit in the measured directions.

For copper this method has been utilized by Svensson *et al.*[1] at room temperature and by Nicklow *et al.*[2] at 49 and 298 K. Their dispersion curves, which are in close agreement with each other, were analyzed in terms of Born–von Kármán models under the assumption of, in part, axially symmetrics (AS) forces. The AS model for metals was originally proposed by Lehman *et al.*[3] and applied to Al and Cu. They compared their theory with thermal diffuse x-ray scattering experiments by Walker[4] for Al and by Jacobsen[5] for Cu, and found for both metals that forces of this type could satisfactorily describe the experimental data. When more reliable experimental results were available for Al (by Yarnell *et al.*[6] and by Stedman and Nilsson[7]), these were analyzed for the symmetry directions by Gilat and Nicklow and good agreement was obtained with an axially symmetric eighth-nearest-neighbor model.[8] It turned out, however, that this parameter set did not satisfactorily produce frequencies in off-symmetry directions[9] and a much better agreement over the whole Brillouin zone for aluminum is obtained when general forces are used and when the complete set of phonons by Stedman and Nilsson is used in the fitting procedure.[10] This shows that a short-range AS model can give a

good fit for metals in the main symmetry directions while there are considerable discrepancies between model and experiment for phonons in off-symmetry directions. To check the validity of specific force-constant model, it is therefore necessary to compare the predictions of the model with measured phonon frequencies in the whole Brillouin zone.

Sinha[11] used the time-of-flight technique to obtain the dispersion relations in copper. Most of the measured phonons have wave vectors outside the symmetry directions. They are limited to, and unevenly distributed in, the (100) and (110) planes. The force-constant model derived from these measurements on the assumption of general forces was in close agreement with models by Svensson *et al.* obtained from more accurate measurements in symmetry directions and on the assumption of, in part, axially symmetric forces. It was found, however, in a comparison of different models, that the AS condition was not exactly fulfilled.[1]

II. EXPERIMENTAL

Phonon frequencies have been obtained for all wave vectors $(2\pi/a)$ (n_1, n_2, n_3), where $n_i = 0.0$, 0.1, 0.2, $\ldots$, 1.0, and a is the lattice constant. On account of the symmetry conditions these are reduced to 146 nonequivalent wave vectors. About one-third of these phonons were measured; the others were interpolated graphically.[9] Such a mesh of points contains sufficient information for determination of general forces in an eighth-nearest-neighbor model, and it also provides a means of checking this model in the whole reciprocal space.

The measurements were performed on a three-axis crystal spectrometer at the R2 reactor at Studsvik. The instrument has been described elsewhere,[12] and we shall only mention some characteristic properties. The sample was situated in a cryostat and cooled with liquid nitrogen to 80 K. In order to make it easy to measure phonons not confined to a single plane, the sample could be turned

around a horizontal as well as a vertical axis. These and all other movements of the instrument were automated and controlled by a punched tape. A computer calculated the settings of the spectrometer together with momentum and energy resolution.[13] The constant-κ method[14] was consistently used. As monochromator we utilized Cu (220) [in a few cases Cu (420)] and as analyzers Cu (220) and Cu (111). The horizontal collimation before the sample was 0.007 rad and 0.019 or 0.013 rad after.

The coherent scattering cross section for thermal neutrons (7.3 b) is favorable in copper, but the absorption (3.8 b) is somewhat disturbing. The sample was a slab 0.9 ×5.5 ×12 cm cut from a cylinder and with a mosaic spread of 0.1°. All phonon resonances were obtained by observing phonon creation.

III. RESULTS

In Table I the phonon frequencies are given for a set of wave vectors in the irreducible part of the Brillouin zone. The average error is estimated to be 0.04 THz, but individual errors may be about twice this value. From geometrical interpolation curves we have constructed the equienergy surfaces on the boundary of an elementary tetrahedron in the reciprocal space. These are shown in Figs. 1(a), 1(b), and 1(c) for the branches T_1, T_2, and L, respectively, where T_1 represents the lowest, T_2 the intermediate, and L the highest energy.

The phonon-dispersion curves are shown in Fig. 2 for the symmetry directions and for some lines on the boundary of the Brillouin zone. The slopes of the branches at Γ are in close agreement with values calculated from elastic constants.

A. Force Constants

Born–von Kármán models are often fitted to measured dispersion curves in metals, although it is well known that these models are not physically satisfactory, because they do not take the full interactions of the conduction electrons into account. Despite their defects these models offer a valuable method for fitting curves to experimental data. As a rule only results for the symmetry directions are used. In these directions the phonon-frequencies-squared depend linearly on the force constants, which is not the case for a general point in the Brillouin zone. Having a force-constant model for the fcc structure extending to the fourth nearest neighbor, it is possible to calculate all parameters from measurements in the symmetry directions only. When the AS condition is added, one can include more remote neighbors and a better fit for the symmetry directions may be obtained. But how well all these models work at points off the symmetry directions may not, of course, be known until these frequencies are measured.
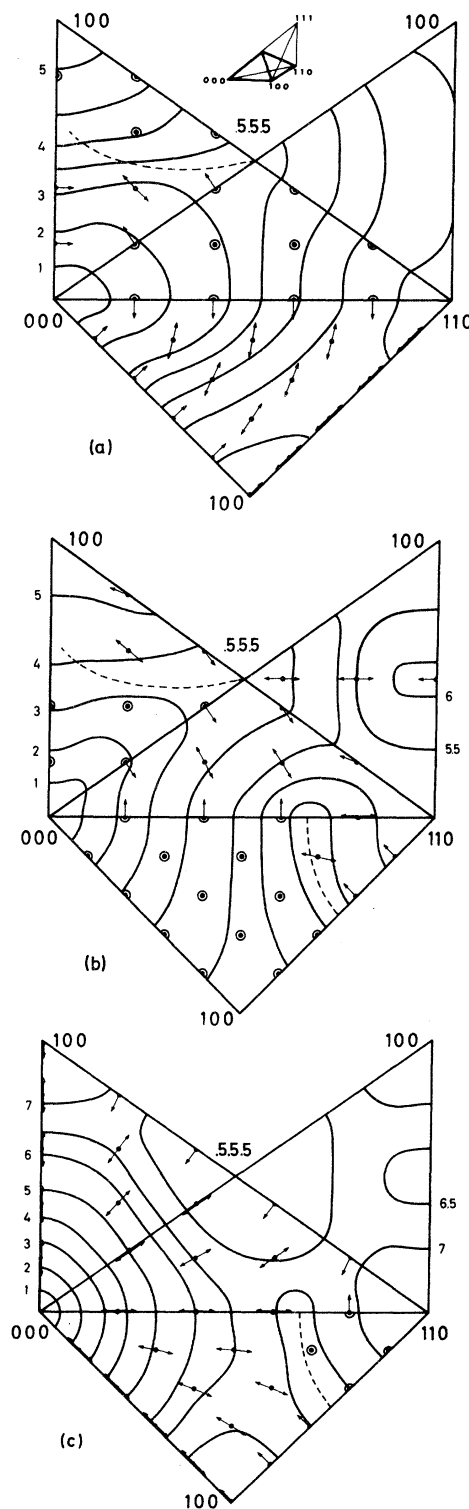
FIG. 1. Equienergy surfaces on the boundary of an elementary tetrahedron. The indicated polarization directions are calculated from the eighth-nearest-neighbor Born–von Kármán model. The low-energy branch T_1, the intermediate-energy branch T_2, and the high-energy branch L are shown in (a), (b), and (c), respectively. Dashed lines indicate accidental degeneracies.

TABLE I. Phonon frequencies in copper at 80 K for a complete set of wave vectors. Underlined frequencies are measured.

10q			ν_1	ν_2	ν_3
0	0	1	0.83	0.83	1.25
0	0	2	1.68	1.68	2.46
0	0	3	2.41	2.41	3.55
0	0	4	3.12	3.12	4.52
0	0	5	3.71	3.71	5.42
0	0	6	4.23	4.23	6.16
0	0	7	4.64	4.64	6.66
0	0	8	4.96	4.96	7.08
0	0	9	5.10	5.10	7.28
0	0	10	5.16	5.16	7.38
0	1	1	0.71	1.20	1.98
0	1	2	1.35	1.89	2.80
0	1	3	2.15	2.60	3.85
0	1	4	2.95	3.25	4.75
0	1	5	3.60	3.84	5.50
0	1	6	4.12	4.33	6.20
0	1	7	4.54	4.74	6.70
0	1	8	4.85	5.03	7.05
0	1	9	5.06	5.17	7.20
0	1	10	5.14	5.25	7.30
0	2	2	1.37	2.36	3.68
0	2	3	1.92	2.93	4.48
0	2	4	2.62	3.54	5.15
0	2	5	3.38	4.14	5.80
0	2	6	4.00	4.53	6.32
0	2	7	4.42	4.90	6.72
0	2	8	4.77	5.19	6.97
0	2	9	5.00	5.33	7.08
0	2	10	5.07	5.36	7.10
0	3	3	2.06	3.43	5.06
0	3	4	2.56	3.95	5.60
0	3	5	3.17	4.44	6.04
0	3	6	3.85	4.81	6.37
0	3	7	4.32	5.13	6.69
0	3	8	4.70	5.40	6.81
0	3	9	4.91	5.55	6.80
0	3	10	5.00	5.61	6.81
0	4	4	2.75	4.39	5.99
0	4	5	3.17	4.77	6.27
0	4	6	3.75	5.15	6.48
0	4	7	4.23	5.47	6.62
0	4	8	4.62	5.67	6.64
0	4	9	4.86	5.81	6.55
0	4	10	4.93	5.90	6.50
0	5	5	3.39	5.16	6.50
0	5	6	3.80	5.50	6.59
0	5	7	4.24	5.80	6.57
0	5	8	4.58	6.01	6.45
0	5	9	4.84	6.15	6.26
0	5	10	4.88	6.18	6.18
0	6	6	3.93	5.85	6.51
0	6	7	4.23	6.14	6.37
0	6	8	4.60	6.16	6.35
0	6	9	4.84	5.97	6.46
0	7	7	4.40	6.13	6.45
0	7	8	4.66	5.88	6.68
0	7	9	4.90	5.70	6.76
0	8	8	4.80	5.66	6.94
0	8	9	5.02	5.47	7.06
0	9	9	5.11	5.33	7.29

TABLE I. (Continued)

10q			ν_1	ν_2	ν_3
1	1	1	1.02	1.02	2.46
1	1	2	1.45	1.68	3.28
1	1	3	2.18	2.40	4.13
1	1	4	2.94	3.05	4.92
1	1	5	3.65	3.69	5.68
1	1	6	4.15	4.29	6.30
1	1	7	4.59	4.73	6.75
1	1	8	4.87	5.07	7.02
1	1	9	5.03	5.25	7.22
1	2	2	1.52	2.15	4.05
1	2	3	2.06	2.74	4.69
1	2	4	2.65	3.30	5.39
1	2	5	3.43	3.91	5.92
1	2	6	4.03	4.43	6.42
1	2	7	4.41	4.86	6.77
1	2	8	4.75	5.19	6.98
1	2	9	4.94	5.43	7.07
1	3	3	2.15	3.23	5.27
1	3	4	2.58	3.78	5.76
1	3	5	3.24	4.26	6.18
1	3	6	3.86	4.68	6.59
1	3	7	4.29	5.11	6.84
1	3	8	4.62	5.39	6.95
1	3	9	4.81	5.63	6.90
1	4	4	2.79	4.12	6.20
1	4	5	3.20	4.53	6.48
1	4	6	3.74	4.97	6.69
1	4	7	4.23	5.34	6.80
1	4	8	4.56	5.62	6.75
1	4	9	4.75	5.83	6.58
1	5	5	3.37	4.90	6.68
1	5	6	3.80	5.28	6.73
1	5	7	4.21	5.63	6.71
1	5	8	4.55	5.87	6.63
1	5	9	4.75	6.05	6.40
1	6	6	3.87	5.57	6.70
1	6	7	4.23	5.84	6.67
1	6	8	4.55	5.91	6.62
1	7	7	4.38	5.86	6.66
1	7	8	4.61	5.72	6.78
1	8	8	4.77	5.55	6.99
2	2	2	1.91	1.91	4.60
2	2	3	2.27	2.42	5.20
2	2	4	2.84	3.00	5.80
2	2	5	3.52	3.54	6.25
2	2	6	4.04	4.24	6.60
2	2	7	4.38	4.88	6.81
2	2	8	4.66	5.32	6.96
2	3	3	2.38	2.86	5.72
2	3	4	2.80	3.31	6.18
2	3	5	3.35	3.80	6.50
2	3	6	3.80	4.36	6.78
2	3	7	4.21	4.94	6.89
2	3	8	4.47	5.40	6.93
2	4	4	2.89	3.73	6.55
2	4	5	3.27	4.11	6.77
2	4	6	3.72	4.55	6.92
2	4	7	4.17	5.04	7.02
2	4	8	4.41	5.51	6.91
2	5	5	3.41	4.43	6.96
2	5	6	3.73	4.78	7.03
2	5	7	4.10	5.16	7.01

TABLE I. (Continued)

10q			ν_1	ν_2	ν_3
2	5	8	4.38	5.52	6.85
2	6	6	3.90	4.99	7.06
2	6	7	4.18	5.24	7.01
2	7	7	4.29	5.36	6.94
3	3	3	2.72	2.72	6.24
3	3	4	2.98	3.03	6.63
3	3	5	3.44	3.46	6.88
3	3	6	3.81	4.08	7.05
3	3	7	4.09	4.76	7.08
3	4	4	3.05	3.32	6.94
3	4	5	3.34	3.70	7.07
3	4	6	3.69	4.15	7.13
3	4	7	3.95	4.70	7.12
3	5	5	3.46	3.96	7.20
3	5	6	3.68	4.20	7.18
3	5	7	3.99	4.60	7.15
3	6	6	3.78	4.44	7.22
4	4	4	3.23	3.23	7.16
4	4	5	3.40	3.43	7.26
4	4	6	3.62	3.86	7.31
4	5	5	3.43	3.54	7.34
4	5	6	3.55	3.80	7.30
5	5	5	3.41	3.41	7.44

Squires[15] pointed out that if the forces are effectively zero beyond a certain limited distance, it is in principle possible to obtain all force constants from a fit to the frequencies in the whole Brillouin zone. Otherwise it is necessary to know also the polarization of the phonons.[16]

Born–von Kármán models for general forces extending up to the eighth nearest neighbors were fitted to the frequencies in Table I by a procedure of successive approximations. We started with a nearest-neighbor model and made a least-squares fit to the experimental frequencies. Starting values for the parameters were obtained from the elastic constants. One neighbor in turn was added to the model and a new fit was made in each case. From the third-nearest-neighbor model the agreement with experiment improved only slowly. Table II gives values of the force constants for the best fit. In Fig. 2 the first-neighbor model is represented by the dashed curve. The average deviation from the energies in Table I is 1.5%. The full line is for the eighth-nearest-neighbor model for which the deviation is 0.6%.

The eighth-nearest-neighbor model was also fitted to measured phonons only, and from the resulting force constants new values for the geometrically interpolated frequencies were calculated. The agreement between the interpolated phonon frequencies obtained from these two methods was quite satisfactory.

One of our purposes in constructing the force-constant model was to use its inability to give a good fit at the Kohn anomalies[17] for an investigation of these. The Kohn effect in copper is very weak but possible to observe.[18] The exact position and size of these small kinks may, however, be rather difficult to point out, as one does not know exactly how the dispersion curves and their gradients would vary with the anomaly absent. We hope that the model derived may be of use in this respect.[19]

For comparison, an AS model was derived where the fitting was restricted to frequencies in the symmetry directions [100], [110], [111], and [0, 1, ξ]. The force constants obtained are pre-
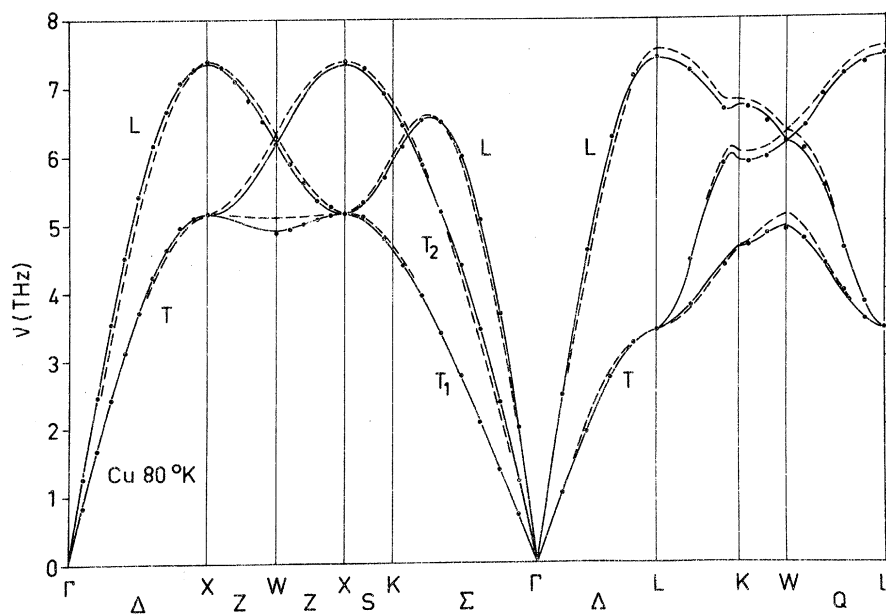
FIG. 2. Dispersion curves for Cu at 80 K. The dashed curves represent the first-nearest-neighbor model and the solid lines the eighth-nearest-neighbor model. (The fit is made to all points in Table I.)

sented in Table II. The mean deviation for all frequencies in Table I was for this model 0.8%, and the deviation remained the same when all the frequencies of Table I were included in the fit. The same agreement was obtained with four nearest neighbors in the general model.

The limits of errors for the parameters presented are somewhat questionable, because a good fit may also be obtained with other parameter sets, but we estimate the errors to be of the order of 100 dyn/cm.

B. Phonon Frequency Distribution and Heat Capacity

The phonon frequency distribution in copper has been calculated from our experimental data by two

TABLE II. Best-fit eighth-neighbor model with general forces.

| Neighbor | Location | | Force constant (dyn/cm) $T=80$ K | |
			General forces	AS model
1	(1, 1, 0)	a_1^1	13 570	13 751
		a_3^1	$-1\,078$	$-1\,615$
		b_3^1	15 542	15 366
2	(2, 0, 0)	a_1^2	199	7
		a_2^2	-209	-82
3	(2, 1, 1)	a_1^3	442	711
		a_2^3	315	224
		b_1^3	113	162
		b_2^3	217	325
4	(2, 2, 0)	a_1^4	112	42
		a_3^4	-100	-175
		b_3^4	226	217
5	(3, 1, 0)	a_1^5	-223	-276
		a_2^5	-20	-18
		a_3^5	-186	14
		b_3^5	84	-97
6	(2, 2, 2)	a_1^6	-141	-119
		b_1^6	-126	-185
7	(3, 2, 1)	a_1^7	22	68
		a_2^7	100	32
		a_3^7	-31	10
		b_1^7	-6	15
		b_2^7	-40	22
		b_3^7	34	44
8	(4, 0, 0)	a_1^8	16	14
		a_2^8	123	-58
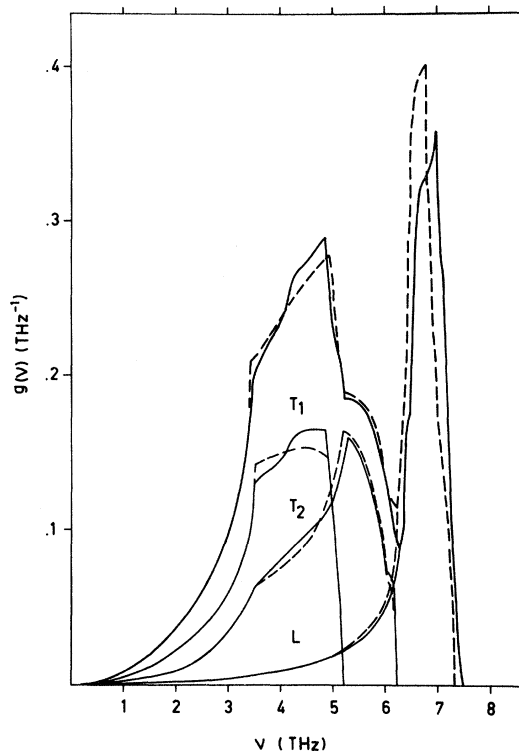
FIG. 3. Phonon frequency distribution from this experiment (solid line) compared with that recalculated from the AS force-constant model at 49 K by Nicklow et al. (Ref. 2) (dashed line). The contributions from low-, intermediate-, and high-energy phonon branches T_1, T_2, and L are also indicated.

different methods. In the method due to Stedman et al.,[9] the phonon frequencies at 10^6 different q values in a quarter of the Brillouin zone were calculated by a second-order Taylor expansion. The coefficients needed to perform the expansion were calculated from the phonon frequencies in Table I. A total of 3×10^6 phonon frequencies were obtained and these were sorted according to energy in a histogram with channel width 0.05 THz. This particular value was chosen to obtain small statistical fluctuations and still retain good resolution. The result is shown in Fig. 3, where the spectrum is somewhat smoothed. The individual contributions from the low- intermediate-, and high-energy branches are also shown.

Figure 4 shows two frequency distributions calculated due to a method of Gilat and Raubenheimer.[20] In this case the two Born–von Kármán models presented in Table II were used for the calculation of the frequency spectra.

From the two-phonon frequency distributions in Fig. 4 the heat capacity and the Debye temperature Θ_D were calculated in the harmonic approximation, in the temperature interval 0–300 K. The tempera-
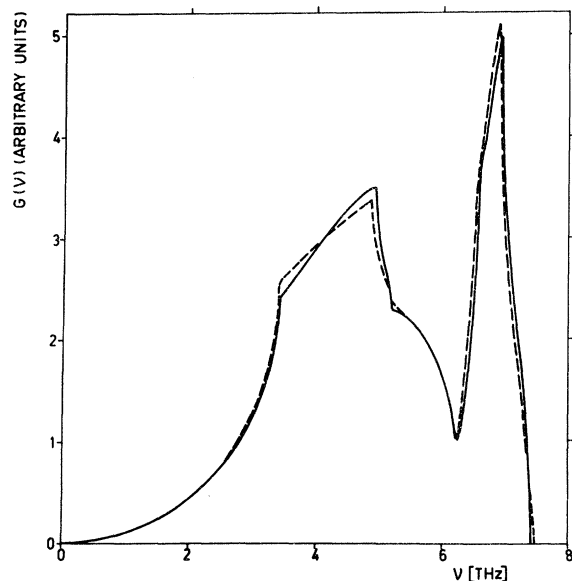
FIG. 4. Phonon frequency distributions calculated from the Born—von Kármán models. Full line is for general force model; AS model is dashed.

ture variation of Θ_D is shown in Fig. 5 together with results obtained from calorimetric measurements by Martin[21] and Cetas et al.[22] The anharmonic contribution to the heat capacity at constant volume is assumed to be small, and this is supported by the behavior of Θ_D derived from calorimetric measurements, which shows that the Debye temperature is almost constant in the temperature

range 100–300 K.[21] The agreement between neutron and calorimetric results is very satisfactory but the general force model gives small but significant improvements over the AS model, as far as the temperature variation of the Debye temperature is concerned. The frequency distribution in Fig. 3 contains a systematic error for small frequencies, which causes an error in Θ_D at low temperatures. When this deficiency is corrected, the Debye temperatures obtained from this spectrum are also in good agreement with the calorimetric experiments.

IV. COMMENTS

Our results are mainly for nonsymmetry directions, as the other frequencies are well known from other measurements, but several phonons in symmetry directions have also been measured for comparison. The agreement between our frequencies and those measured by Nicklow et al.[2] at 49 K is generally very good, although we got somewhat higher values for the most energetic longitudinal phonons. Nicklow et al. studied the widths of some phonons at 49 and 298 K. For $q = 0.9$ in the 100 L branch they found phonons with a width of 18% at both temperatures. With a Cu (420) monochromator and Cu (220) analyzer we obtained an estimated energy resolution of 3.0% for that phonon, and the observed width was 3.4%, which means that the intrinsic width is probably less than 2% at 80 K. For the corresponding transverse phonon our resolution was 2.4%, the width of the observed peak 3.0%, and the real phonon width about 1%. At both 49 and 298 K the widths for this transverse
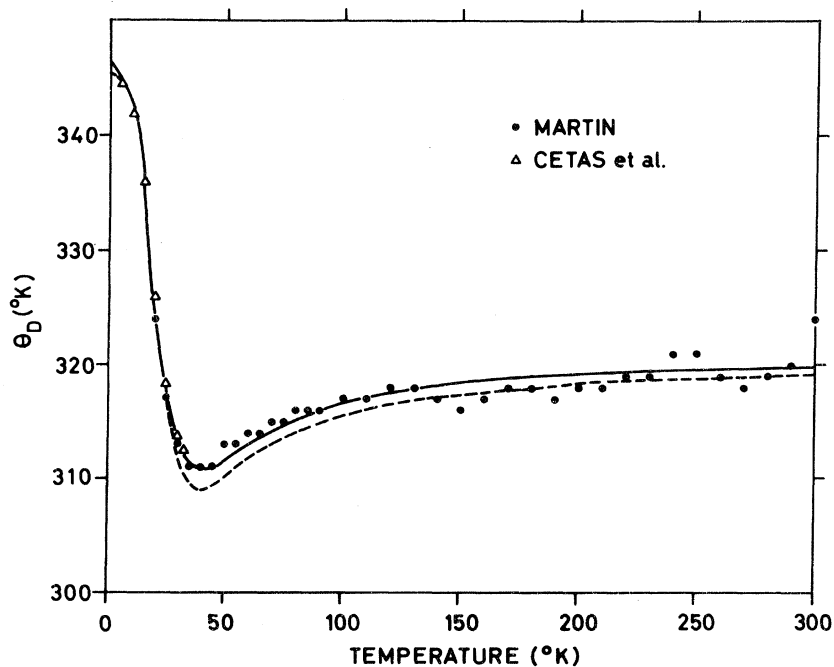
FIG. 5. Debye temperature as calculated from the two frequency distributions in Fig. 4 according to the harmonic theory. Comparison is made with calorimetric experiments.

phonon shown in Ref. 2 were 10%, which, there-fore, was probably the instrumental resolution in that case.

In the frequency distribution derived from these measurements the Van Hove singularity[23] at $\nu = 3.5$ THz observed by Sinha,[11] Svensson et al.,[1] and Nicklow et al.[2] has become more obtuse. This originates from the behavior of the low-energy branch T_1. With the method used to obtain the spectra in Fig. 3, we have recalculated the frequency distribution from Nicklow's force constants at 49 K as well as the separate contributions from the three branches. These are indicated by dashed lines on Fig. 3.

The height of the low-frequency part is depressed at 3.7 THz and increased at 4.7 THz in our frequency distribution, compared with the one by Nicklow et al. The same effect is observed in Fig. 4, where the general force model and the AS model are compared. The shape of the spectrum derived from the model by Sinha has in this respect a closer similarity with our frequency distribution than the others. This may reflect the fact that nonsymmetry phonons from the (100) and (110) planes were used in his model. Bührer has recently measured dispersion curves for some lines within the Brillouin zone at room temperature and also obtained a similar frequency distribution from his model.[24]

Nicklow et al. measured the temperature dependence of the phonon frequencies between 49 and 298 K, and Miiller and Brockhouse[25] measured the frequency shifts as a function of temperature above room temperature, and extrapolated to the range below room temperature for the mean phonon frequency shift, obtaining a somewhat larger value than Nicklow et al. From Eq. (8) in Ref. 25, we calculated the mean frequency shift with temperature at constant volume and constant pressure, respectively, using the heat-capacity data of Martin[21] and the harmonic heat capacity calculated from our

spectra. The average phonon frequency shift between 80 and 300 K was calculated to 1.9% for constant pressure, which is in good agreement with the data of Miller and Brockhouse. The shift at constant volume was, however, found to be no more than 0.1%. This indicates that copper is a metal where the quasiharmonic approximation is quite suitable, i.e., where the frequencies depend only on volume.

Our high-energy peak is shifted towards higher frequencies relative to that of Nicklow et al. at 49 K, since our longitudinal dispersion curves rise to higher energies. The over-all agreement between our frequency distribution and that of Nicklow et al. for Cu is, however, much better than the agreement between the corresponding distributions obtained for Al by Stedman et al. and by Gilat and Nicklow. The latter derived their frequency distribution for Al by using an AS model based on experimental results in the symmetry direction reported by Stedman and Nilsson. In this fit the $[1, \xi, 0]$ direction was not included. The Al results have, however, recently been treated in the same way as the copper results[10] in a comparison where all figures are comparable. The root-mean-square deviation for all frequencies in copper (aluminum) was for the AS model 0.045 THz (0.13 THz). When all frequencies were included in the fit this deviation was reduced to 0.040 THz (0.10 THz). For the general force model the corresponding figure is 0.031 THz (0.047 THz). From an analysis of force constants derived for the two metals and from a comparison of how well different models work in the Brillouin zone, we conclude that the AS model is definitely more suitable for Cu than for Al, although for copper the general force model is also preferable.

[1]E. C. Svensson, B. N. Brockhouse, and J. M. Rowe, Phys. Rev. 155, 619 (1967).

[2]R. M. Nicklow, G. Gilat, H. G. Smith, L. J. Raubenheimer, and M. K. Wilkinson, Phys. Rev. 164, 922 (1967).

[3]G. W. Lehman, T. Wolfram, and R. E. De Wames, Phys. Rev. 128, 1593 (1962).

[4]C. B. Walker, Phys. Rev. 103, 547 (1956).

[5]E. H. Jacobsen, Phys. Rev. 97, 654 (1955).

[6]J. L. Yarnell, J. L. Warren, and S. H. Koenig, in Proceedings of the International Conference on Lattice Dynamics, Copenhagen, 1963, edited by R. F. Wallis (Pergamon, Oxford, England, 1965), p. 57.

[7]R. Stedman and G. Nilsson, Phys. Rev. 145, 492 (1966).

[8]G. Gilat and R. M. Nicklow, Phys. Rev. 143, 487 (1966).

[9]R. Stedman, L. Almqvist, and G. Nilsson, Phys. Rev.

162, 549 (1967).

[10]G. Nilsson (unpublished).

[11]S. K. Sinha, Phys. Rev. 143, 422 (1966).

[12]R. Stedman and G. Nilsson, Rev. Sci. Instrum. 39, 637 (1968).

[13]R. Stedman, Rev. Sci. Instrum. 39, 878 (1968).

[14]B. N. Brockhouse, in Phonons in Perfect Lattices and in Lattices with Point Imperfections, edited by R. W. H. Stevenson (Oliver and Boyd, Edinburgh, 1966), p. 110.

[15]G. L. Squires, Arkiv Fysik 25, 21 (1963).

[16]A. J. E. Foreman and W. M. Lomer, Proc. Phys. Soc. (London) 70, 1143 (1957).

[17]G. Dolling and A. D. B. Woods, in Thermal Neutron Scattering, edited by P. A. Egelstaff (Academic, London, 1965), p. 204.

[18]G. Nilsson, Proceedings of the Conference on Neutron Inelastic Scattering, Copenhagen, 1968 (International Atomic Energy Agency, Vienna, 1968), Vol. I, p. 187.

[19]G. Nilsson and S. Rolandson (unpublished).

[20]G. Gilat and L. J. Raubenheimer, Phys. Rev. 144, 390 (1966).

[21]D. L. Martin, Can. J. Phys. 38, 17 (1960).

[22]T. C. Cetas, C. R. Tilford, and C. A. Swenson, Phys. Rev. 174, 835 (1968).

[23]L. Van Hove, Phys. Rev. 89, 1189 (1953).

[24]W. Bührer, Eidgenoessisches Inst. fuer Reaktorforschung Report No. 174, Würenlingen, Switzerland, 1970 (unpublished).

[25]A. P. Miller and B. N. Brockhouse, Can. J. Phys. 49, 704 (1971).

Giant Quantum Oscillations in the Magnetoacoustic Attenuation of Mercury*

G. Bellessa

Laboratoire de Physique des Solides,[†] Bâtiment 510, Faculté des Sciences, 91-Orsay, France

(Received 2 August 1972)

Measurements of the magnetoacoustic attenuation have been performed in mercury single crystals at temperatures down to 0.45 K and fields up to 70 kOe. For longitudinal waves in the frequency range 20–70 MHz, the attenuation coefficient exhibits giant quantum oscillations with spikelike character. The attenuation peaks are induced by the β arms of the first-zone hole surface. Their period in inverse magnetic field is measured as a function of the magnetic field orientation. The particular shape of the attenuation peaks is explained by taking into account the negative value of the effective mass in the magnetic field direction (saddle point). Measurements of the linewidth and height are presented. It is shown that the line suffers an inhomogeneous broadening. The latter is connected with the effect of dislocations on the Landau levels and a line-shape calculation is presented. Unusual line-height properties are reported. The line height depends on the ultrasonic-wave amplitude and in some cases there are attenuation dips instead of attenuation peaks at the same magnetic field values. The peak-height behavior is explained by a magnetic field effect on the electron-dislocation interaction.

I. INTRODUCTION

The giant quantum oscillations (GQO) in the magnetoacoustic attenuation in metals have been predicted by Gurevitch et al.[1] According to the theory, the GQO are peaks in the acoustic attenuation versus magnetic field. The latter arise from the resonant absorption of the sound wave by the electrons which move along the magnetic field with the sound velocity (in the simplest case where the wave vector is parallel to the magnetic field). The GQO have been observed in zinc,[2,3] rhenium,[4] bismuth,[5-8] gallium,[9] arsenic,[10] and mercury,[11] but it is only in the four last materials that the GQO exhibit a spikelike character. By studying the shape of the attenuation peaks, one can obtain information about the cyclotron mass, the g factor, and the relaxation time. It is the purpose of this paper to report the results of such a study in mercury.

The main parts of the paper are Sec. II, a brief description of the GQO theory and new theoretical calculations about the line shape; Sec. III, a description of the experimental procedure; Sec. IV, the presentation of the experimental results; and Sec. V, the interpretation of some GQO-peak properties with a magnetic field effect on the electron-dislocation interaction.

II. THEORY

The GQO theory has been established by Gurewitch et al.[1] for the free-electron case. In the case of mercury, we shall deal with quasicylindrical Fermi surfaces. Therefore, we refer in this part to the theory of Kaner and Skobov,[12] who have taken a nonisotropic energy-momentum law for the electrons. One can write for the electron energy in the presence of an uniform magnetic field $\vec{H}$ along the z axis

$$E_n(k_z) = n\hbar\Omega + \hbar^2 k_z^2/2m_\| , \tag{1}$$

where n is the Landau-level number, Ω is the cyclotron frequency $eH/m_c c$, and k_z is the z component of the electron wave vector. The effective mass $m_\|$ in the magnetic field direction is defined by the relation

$$\frac{1}{m_\|} = \frac{1}{\hbar}\left(\frac{\partial}{\partial k_z}\langle v_z\rangle_{\text{av}}\right)_0 = \frac{1}{2\pi m_c}\left(\frac{\partial^2 A}{\partial k_z^2}\right)_0 , \tag{2}$$

where $A(k_z)$ is the area of the intersection of the Fermi surface with a plane perpendicular to $\vec{H}$. We omit index k_y in Eq. (1) because the energy does not depend on this quantum number. Nevertheless, we take it into account when we replace the sum over states by an integral. For simplicity, we have written neither the spin term nor the phase term